

MAP-MATCHING OF RADAR IMAGES AND ELECTRONIC CHARTS USING THE HAUSDORFF DISTANCE

Tzu C. Shen and Andrés R. Guesalaga

Department of Electrical Engineering, Catholic University of Chile, 4860 Vicuna Mackenna, Casilla 306-22, Santiago, Chile

Keywords: Map-matching, pattern recognition, radar calibration

Abstract: This paper describes a new method of image pattern recognition based on the Hausdorff Distance. The technique looks for similarities between a given pattern and its possible representations within an image. This method performs satisfactorily when confronted to image perturbations or partial occlusions. An extension of the classical Hausdorff Distance technique chooses the best candidate among multiple sub-optimal solutions. The search strategy is based on the Branch and Bounds algorithm, where cells with low probability of containing the optimal solution are pruned, while feasible cells are divided again until the optimal solution is found. By using this strategy, exhaustive and no-informative searches are avoided among the possible combinations, reducing the processing time considerably. A case study is presented, where the proposed method is applied to calibration of surveillance radars using hydrographic charts as models for the radar echo images.

1 INTRODUCTION

It has been suggested that approximately 8%-10% of vessels are now fitted with some form of electronic chart systems (ECS) (Bailey, 2001). Furthermore a standardization in chart formatting has been observed in the last decades, where the International Hydrographic Organisation has played a major role developing the S57 standard for digital hydrographic data transfer (IHO, 2000).

The integration of ECS and radar scan images is becoming a must in navigation consoles and it can be used for purposes other than navigation. In this paper, the use of integrated imagery obtained from navigation radars and ECS is addressed by proposing an automatic map-matching technique to estimate biases of radars and remove them from range and bearing measurements. The aim of such technique is to improve the accuracy of these monitoring system, i.e. navigation, target designation and surveillance among others.

This tool can be particularly useful for track-to-track association procedures and track fusion (Hall and Garga, 1999), where multiple sensors interchange information of radar contacts but each with deviations caused by factors such as difference in sampling periods, sensor noise and distortions caused by biases in range and bearing

measurements. It is mandatory for such systems to reduce these kind of errors to a minimum, so a simple technique to perform periodic calibrations of these biases would be welcomed.

In modern navigation systems, an additional problem arises due to the vulnerability of GPS to spoofing or satellite denial. This is a matter of particular concern in countries that do not conform the military elite (Taylor, 2003).

Previous work in map-matching has been reported in the literature, mainly for airborne systems. In a previous work (Wilson et al, 1995), a discrete relaxation technique is used for registering incomplete radar images acquired from synthetic aperture radars. They use a maximum-likelihood technique to match Doppler beam sharpened images to digital maps of rural terrain. Although these techniques are related to the scope of this paper, they differ in that the data is a sequence of non-overlapping radar sweeps interspersed with substantial dead-regions. Furthermore, the application does not require precise calibration of the radar in terms of range and bearing offsets, and the problem of distorted regions is not an issue. A novel technique based on the extended Kalman filter has been recently proposed to estimate these offsets (Guesalaga, 2003). By defining at least two corresponding points from the radar image and the

electronic chart, the technique provides a rapid and accurate calibration in range and bearing, giving also estimates for the ship's speed, heading, latitude and longitude. It does not require GPS nor speed information from the ship log unit. The method, however, relies on the operator to detect and select the corresponding points between the electronic chart and the radar image. This is a major disadvantage, since he has to disregard other more important functions, is prone to introduce significant errors and his performance can be affected by fatigue.

The main objective of this work is the development of a pattern recognition algorithm to detect similarities between the radar measurements and the model, represented by the electronic chart. This will allow to find the corresponding points between the two sets of data automatically.

The nature of the reference set (electronic charts) restricts the possible approaches to techniques based on models. Among them, some well-established methods are those based on correspondences (Anandan, 1989), correlation (Brock-Gunn and Ellis, 1992) and exact methods (Fredriksson et al, 2002). There are other less popular techniques based on previous knowledge of the domain (Worrall et al, 1991), heuristics (Yuille et al, 1992) or contextual (Prokopowicz, 1994).

Most of these methods do not perform satisfactorily for the problem stated, because objects can be totally or partially occluded or they can have important distortions due to the polar nature of the measurement (radar scans). Exact techniques or those that rely on rigid or previously known models for search, have to be discarded. These restrictions are liberated in correspondence techniques that are based on the Hausdorff Distance (Sim and Park, 2001). Furthermore, the problem of semi-occluded objects and distortions are solved via extensions of the latter technique, i.e. the so called Partial Hausdorff Distance (Rucklidge, 1977) and the extensions to the algorithm proposed in the following sections.

1.1 The Hausdorff Distance (HD)

This technique is based on a rather "loose" approach of looking for similar objects, instead of trying to correlate pair of points in two images. By taking two sets of points, one being the model and the other the real image, the HD between them is small when every point in one of the sets is near to some point in the other image.

Figure 1 shows a geometric representation of the HD when used for pattern recognition. Here sets A

and B are the model and real image respectively and by rotating and translating the model, a satisfactory matching is obtained.

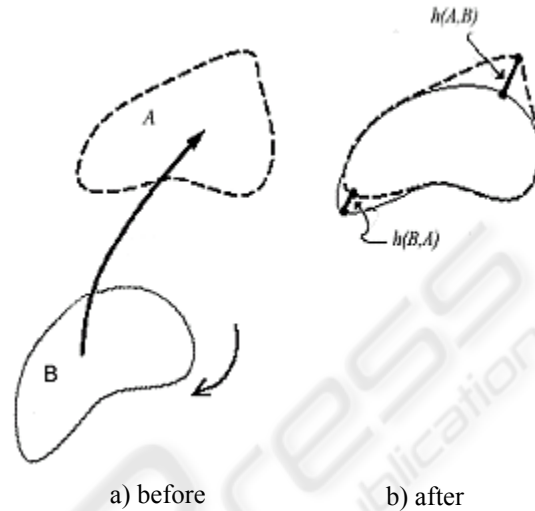


Figure 1: Geometric representation of the HD, before and after transformation

Given two sets with a finite number of points, $A = \{a_1, a_2, \dots, a_p\}$ and $B = \{a_1, a_2, \dots, a_q\}$, the Hausdorff Distance between A and B is:

$$H(A,B) = \max(h(A,B), h(B,A)) \quad (1)$$

where,

$$h(A,B) = \max_{a \in A} \min_{b \in B} \|a - b\| \quad (2)$$

$h(A,B)$ is called the standard Hausdorff Distance between sets A and B . The algorithm sorts the points in A according to its distance to the nearest point in B and selects the largest as the result.

For instance, if $h(A,B)=h$, then every point in A is at most at a distance h of a point in B , and the point (with distance h), is the point with the largest deviation. Figure 2 exemplifies the above concept for sets A and B , each containing two and three points respectively. It is important to note that this index is in most cases asymmetric respect to its inverse, i.e. $h(A,B) \neq h(B,A)$.

1.2 Voronoi surface

In practical applications, comparing only two sets of data is not enough, since although the reference pattern can be clearly defined, there are multiple candidates B_i that can be similar to the model A . In order to reduce the number of calculations, the

concept of Distance Transformation (Borgefors, 1986) is introduced. Here, set A is pre-processed to an intermediate state called the Voronoi matrix V (Huttenlocher et al, 1992), for a subsequent matching of the latter matrix with the different candidates B_i . By doing so, set A is processed only once.

From equations (1) and (2), HD can be written as:

$$H(A, B) = \max_{a \in A} \max_{b \in B} d(a), \max_{b \in B} d'(b) \quad (3)$$

where

$$d(x) = \min \|x - b\| \quad \text{and} \quad d'(x) = \min \|x - a\| \quad (4)$$

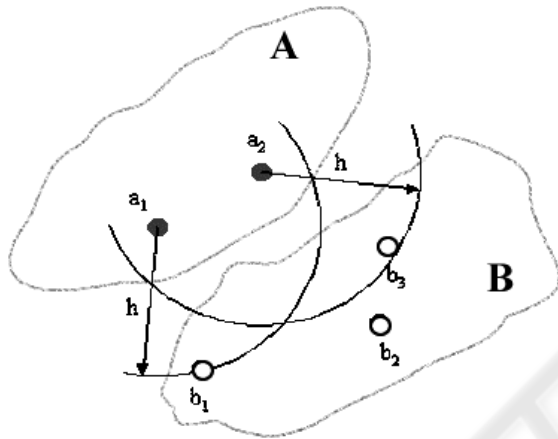


Figure 2: Standard Hausdorff Distance, $h(A,B)$

The function $d(x) = \{x, d(x) | x \in R^2\}$ is called the *Voronoi Surface*, and allows to perform the *Distance Transformation* by filling the points of V with the value d_{max} obtained from matrix A . A detailed description of the algorithm can be found in (Rucklidge, 1997).

1.3 Modifications to the algorithm

Some modifications to the previous algorithm had to be necessary for applications where sets A and B are not identical. This is normally caused by occlusions, measurement noise and image distortions caused by the technique used the image acquisition. The latter is particularly valid for radar images where the measured set is obtained in polar co-ordinates, so errors in range will cause a shrinkage or enlargement of the objects. Sometimes these differences can be also introduced in the intermediate stages such as edge detection, expansion, rotation, translation and others. To reduce the impact of these error sources, some further steps are introduced in the method and

they are briefly described in the following paragraphs.

Partial Hausdorff Distance

The above mentioned sources of error will generate some false-positive points with a distance significantly larger than the one of any true-positive point. In order to eliminate the negative impact of those points on the HD calculation, the method chooses the j^{th} distance instead of the largest one. The rejection of the largest values can imply losing information, however, the effect is negligible when considering the whole sets A and B , and the improvement in the robustness of the method is significant.

Mathematically:

$$h_K(A, B) = K^j \min_{a \in A} \min_{b \in B} \|a - b\|, \text{ for } 1 \leq K \leq n \quad (5)$$

where K^j is the j^{th} farthest distance between the points $a \in A$ and those in B , and n is the number of points in B .

For convenience, the number of points in the remaining set is defined in terms of a ratio of the total set, i.e. $K = k * n$, and $0 \leq k \leq 1$.

Handling Multiple Solutions

When searching for the candidate that gives the best HD , several subsets B_i with similar values may appear. In these cases, some additional processing stages must be included in the procedure. These intermediate stages are:

Inverse Hausdorff Distance (Rucklidge, 1997)

Taking advantage of the asymmetric nature of the HD , in certain cases it is possible to reject false-positives by interchanging the roles of A and B , i.e. $h(B,A)$ is computed. False-positives will tend to give significantly higher values than that of a real solution, so they can be identified and eliminated. Figure 3 shows an example of a false-positive.

The least HD average

When two or more candidates with similar values for $h(A, B_i)$ are found, an effective criteria to select the best set is by looking at their HD average. This implies that in the set chosen, more points in the image will resemble the model.

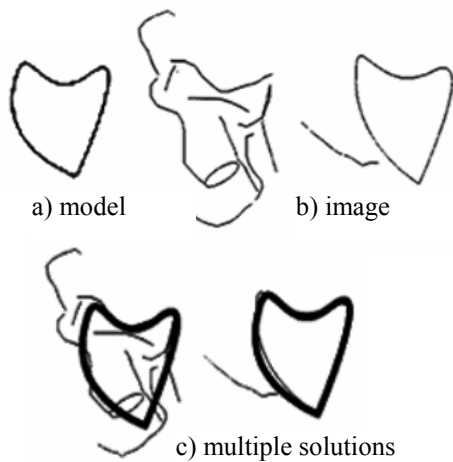


Figure 3: A false-positive case

1.4 The Searching Strategy

The search for the optimal solution is based on the application of a large number of transformations on the image. Some possible transformations or at least those of interest for our application are: translation (Cartesian displacement), rotation (angle) and enlargement (radial distance). The optimal solution would be the result of an image transformation of the three types of transformations listed above, applied over one of the sets, which gives the highest similarity between sets A and B . The number of transformations required in order to test all possible combinations would be prohibitive in terms of processing time if no additional information is provided to the searching procedure. Although it is not in the scope of this work, several searching techniques were tested, and the Branch and Bound method as described in (Breuel, 2003) was selected.

1.5 Edge Detection

In order to reduce the processing time further, images are segmented by applying an edge detector. The method used is the standard Sobel gradient as described by Gonzales and Woods (1993).

2 APPLICATION TO RADAR CALIBRATION

The aim of this application is to calibrate a maritime radar by eliminating biases in bearing and range. Electronic Chart are used to map-match the radar

images obtained with a navigation radar. The matching is made by looking for the optimal combination of basic transformations produced by translation, rotation and range offset.

Due to the vulnerability of GPS systems and their induced errors (when selective availability is turned off), its used is not considered here, so estimation of Latitude and Longitude is also carried out.

A novel method to estimate and correct these errors using the Extended Kalman Filter is described in the literature (Guesalaga, 2003). The method requires that the search for correspondences between the model (chart) and image (radar scan) must be made manually, i.e. the operator has to click over the corresponding points. This makes the method unattractive, so the purpose of this work is to provide a technique to find these correlations automatically, without the intervention from the operator.

2.1 Transformation model

Measurement points can be numerous and sparse. In fact, the larger the number of correspondence points the better the estimation accuracy. The same occurs with the separation of these correspondences, i.e. correspondence pairs covering 360 degrees and stretching along the full distance range should be sought. The transformation model used to match sets A and B is based in a reference system given in polar co-ordinates (due to the nature of the radar scanning) and the actual transformations produce non-rigid displacements of the objects in the image, so their shape is distorted.

For a given point in the radar image, the measuring model is:

$$\begin{aligned} c_{ip} &= (R_i + e_r) \cos(\theta_i + e_\theta) + e_p + n_p \\ c_{iq} &= (R_i + e_r) \sin(\theta_i + e_\theta) + e_q + n_q \end{aligned} \quad (6)$$

where R_i and θ_i are the polar co-ordinates of the point c_i whose origin is given by the ship co-ordinates e_p and e_q . Zero-mean Gaussian noise n_p and n_q are added to account for the errors in measuring correspondences in the radar scan image and they can be influenced by clutter, occlusions or broad radar pulses.

As figure 4 shows, R_i and θ_i define each of the correspondence pairs. Variables e_r and e_θ , in turn, are common to all points selected for matching and they describe the errors in measurements caused by biases in range and bearing respectively. The orientation variable e_θ describes the rotation that suffers the radar image due to disturbances such as misalignments in the position sensors of the antenna (encoders, synchros, etc.), antenna boresight and the

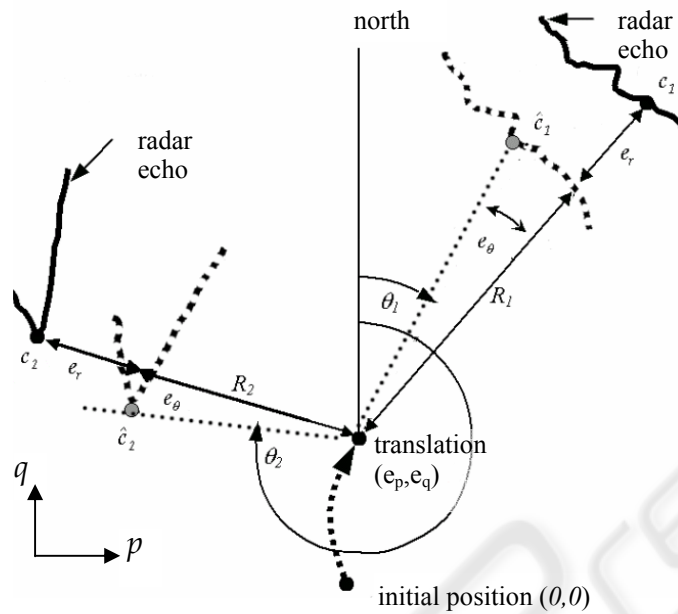


Figure 4: Transformation model.

azimuth error generated by the local level reference frame.

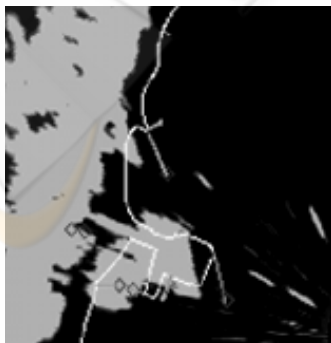
Notice the difference between point c_i , from the radar echo and the one from the chart \hat{c}_i . In order to show the behaviour of the *HD* technique, an example was carried out with radar data collected from a navigation console. An area of 163×170 pixels is processed (see figure 5.a) where the grey zone is the radar echo and the brighter lines correspond to the electronic chart. A notorious mismatch exists between both sets of data. Figure 5.b shows the hydrographic data and figure 5.c the segmented radar image after applying the edge detector. Finally, figure 5.d shows the matching of the two sets after applying the optimal transformation found by the method.



5.b) Electronic chart



5.c) Segmented radar image using edge detector



5.a) Zone of interest: radar image and electronic chart



5.d) Final matching

Figure 5: The different stages in the method

Table 1 contains the values for the optimum transformation. The value found for the Partial Hausdorff Distance is 11 pixels for $k=90\%$, i.e. every point in the radar image considered in the calculations is at most, at a distance of 11 pixels from its corresponding point in the electronic chart.

Table 1: Optimum transformation values

e_r	5.0 pixels
e_θ	3.0 degrees
e_p	17.0 pixels
e_q	-2.0 pixels

Table 2 shows the improvements obtained in the matching. H_o corresponds to the HD before the optimum transformation has been applied. H is the HD when the modified version of the algorithm is applied. Notice the significant improvement obtained in the number of points existing in the range from 0 to 5 pixels (increase of 135%). The HD is also reduced significantly (38%) and the HD average drops by 45%.

Figure 6 shows a distribution graph for the points with correspondences. The curve for the initial HD (H_o , crosses marks) contains less points in the left side of the graphic than the modified HD proposed in this paper (H , circle marks).

Table 2: Comparison of initial situation (H_o) and after transformation (H)

	Initial (H_o)	Final (H)
$d = 0$ pixels	16 points	38 points
$d = 1$ pixel	21 points	66 points
$d = 2$ pixels	21 points	56 points
$d = 3$ pixels	21 points	41 points
$d = 4$ pixels	16 points	37 points
$d = 5$ pixels	21 points	35 points
$d \leq 5$ pixels	116 points	273 points
$HD (k=90\%)$	18 pixels	11 pixels
HD average	11.24 pixels	6.10 pixels

The example shown above must be accompanied by at least one other zone of search for correspondence in order to achieve observability when estimating radar biases (Guesalaga, 2003). In this test, three zones are used.

Figure 7 shows the initial situation for the complete scan of the radar. A miss-match between the radar image and chart is clearly caused not only by linear translations but also by rotation, and a less evident range deformation. After applying the estimation technique described in this paper for the three zones shown in the figure, which in turn feed the Extended Kalman Filter described in Guesalaga (2003) for a sequence of 50 radar scans, the optimum transformation is found and the result is presented in figure 8.

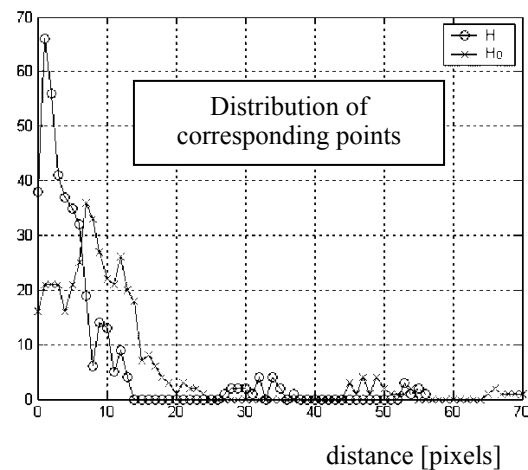


Figure 6: Hausdorff Distance distribution of corresponding points

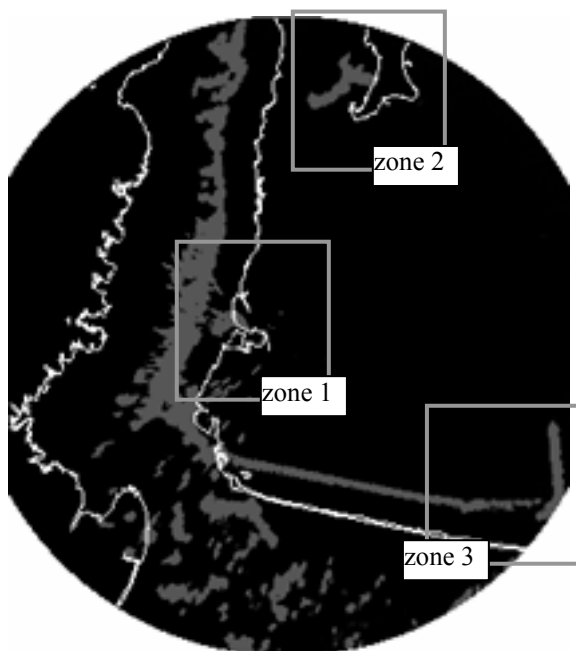


Figure 7: Initial situation



Figure 8: Final matching after optimum transformation

3 CONCLUSIONS

An extended version of the Hausdorff Distance algorithm has been successfully applied to map-matching of radar images and electronic charts.

The method allows to correlate radar images and hydrographic charts automatically in order to detect calibration errors in radar surveillance systems and correct them accordingly.

Several modifications have been introduced to the standard *HD* algorithm showing an excellent performance in terms of reductions in *HD* and greater number of corresponding points in the model being closer to their equivalent points in the image set. Indices such as the actual *HD*, its average and the number of points at distances of less than 5 pixels, showed significant improvements of over 30%, making the proposed technique a very attractive tool for the problem of radar calibration and map-matching.

A critical parameter that needs to be tuned is the *k* ratio, which shortens the sorted list of points in the original image in order to reject false-positive points. This action showed to improve the matching substantially and the reduction in the total data to be processed showed no negative impact on the results.

REFERENCES

- Anandan P., 1989. A computational framework and an algorithm for the measurement of visual motion. *Int. Journal of Computer Vision*. 2:283-312.
- Bailey T., 2001. Electronic chart systems - A bonus or a curse?, *The Hydrographic Journal*, 102:39-52.
- Borgefors, G., 1986. Distances transformations in digital images. *Computer Graphics Images Processing*. 34:344-371.
- Breuel, T.M., 2003. Implementation techniques for geometric branch-and-bound matching methods *Computer Vision and Image Understanding*. 90:258-294.
- Brock-Gunn, S., Ellis, T.J., 1992. Using colour templates for target identification and tracking. *Proc. British Machine Vision. Conf.* pp 207-216. Leeds, UK.
- Fredriksson, K., Navarro, G. and Ukkonen, E., 2002. Optimal Exact and Fast Approximate Two Dimensional Pattern Matching Allowing Rotations. *Proc. of the 13th Annual Symposium on Combinatorial Pattern Matching*. pp 235-248. Fukuoka, Japan.
- Gonzales, R., and Woods, R.E., 1993. *Digital Image Processing*. Addison-Wesley Publishing Company, Reading, Massachusetts. 2nd. edition
- Guesalaga, A.R., 2003. Estimation of Radar Range and Bearing Biases using Electronic Charts. *Proceedings*

- of the SPIE-Aerosense Conference, 5084-19, Orlando, FL.
- Hall D.L., Garga, A.,1999. Pitfalls in data fusion (and how to avoid them). *Proceedings of 2nd Int. Conf. on Information Fusion*, Sunnyvale, CA, July 1999, 1:429-436.
- Huttenlocher, D.P., Kedem, K., and Kleinberg, J.M.,1992. Dynamic Voronoi diagrams and the minimum Hausdorff distance for point sets under Euclidean motion in the plane. *Proc. 8th Annu. ACM Sympos. Comput. Geom.* pp 110-120 .
- IHO, 2000. *Transfer Standard for Digital Hydrographic Data*, Special Publication #57, edition 3.1, Published by the International Hydrographic Bureau, Monaco.
- Prokopowicz, P.N., Swain, M.J. and Kahn, R.E.,1994. Task and environment-sensitive tracking, *Proc. Workshop on Visual Behaviors*. pp 73-78, Seattle, USA.
- Rucklidge, W.J.,1977. Efficient Visual Recognition Using the Hausdorff Distance. *Int. Journal of Computer Vision*. 24:251-270.
- Sim, D.G. and Park, R.H.,2001. Two-Dimensional Object Alignment Based on Robust Oriented Hausdorff Similarity Measure. *IEEE Transactions on Image Processing*. 10:475-483.
- Taylor D.W.,2003. Local area navigation: a tool for GPS-denied geolocation, *Proceedings of the SPIE-Aerosense Conference*, 5084-19, Orlando, FL
- Wilson R.C., Evans A.N., Hancock E.R.,1995. Relational Matching by Discrete Relaxation, *Image and Vision Computing*, 13:411-421.
- Worrall, R.F., Sullivan, and Baker, K.D.,1991. Model-based tracking. *Proc. British Machine Vision. Conf.* pp 310-318. Glasgow, Scotland.
- Yuille, L., Cohen, D.S. and Hallinan P.,1992. Feature extraction from faces using deformable templates. *Int. Journal of Computer Vision* 8:99-112.

